Oxidized Aromatic–Aliphatic Mixed Films at the Air–Aqueous Solution Interface

ARTICLE *in* THE JOURNAL OF PHYSICAL CHEMISTRY C · JUNE 2013

Impact Factor: 4.77 · DOI: 10.1021/jp402737n

5 AUTHORS, INCLUDING:

André S Pimentel

Pontifícia Universidade Católica do Rio de Jan…

46 PUBLICATIONS **371** CITATIONS

SEE PROFILE

THE JOURNAL OF PHYSICAL CHEMISTRY C

Article

pubs.acs.org/JPCC

Oxidized Aromatic–Aliphatic Mixed Films at the Air–Aqueous Solution Interface

Elizabeth C. Griffith,[†] Teobaldo R. C. Guizado,[‡] Andre S. Pimentel,[‡] Geoffrey S. Tyndall,[§] and Veronica Vaida*[,†]

[†]Department of Chemistry and Biochemistry and CIRES, University of Colorado at Boulder, UCB 215. Boulder, Colorado 80309, United States

[‡]Department of Chemistry, Pontificia Universidade Católica do Rio de Janeiro, Gávea, Rio de Janeiro, RJ, 22453-900 Brazil

[§]National Center for Atmospheric Research, P.O. Box 3000, Boulder, Colorado 80307, United States

Supporting Information

ABSTRACT: Mixed organic films composed of molecules with differing hydrophobic groups are relevant to environmental interfaces such as the surface of atmospheric aerosols due to the complex composition of atmospheric emissions. In this work, mixed films composed of oxidized aromatics (benzaldehyde, benzoic acid) and stearic acid are studied using Langmuir trough methods, infrared reflection–absorption spectroscopy (IRRAS), and MD simulations, showing modifications to the surface due to both the hydrophobic and hydrophilic identity of the aromatic molecules. Aromatics are a known component of crude oil, and once released into the atmosphere through an event such as an oil spill, they can be weathered to produce varying degrees of oxidized products like benzaldehyde or benzoic acid. Molecules released through such anthropogenic processes are shown here to have complex interactions with organics released through biogenic emissions (like stearic acid) at the aqueous interface, resulting in diverse surface morphologies that may have an effect on the aerosol particle's overall effect on atmospheric chemistry and climate. The result of these mixed films is discussed in the context of the modern atmosphere.

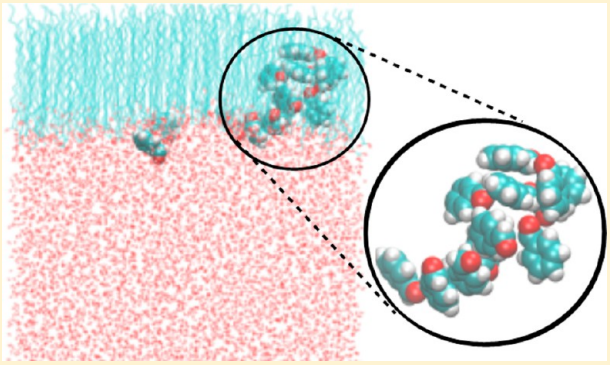

INTRODUCTION

Water surfaces, characteristic of lakes, oceans, and the surface of aqueous atmospheric aerosols, are ubiquitous on Earth and are often rich in organic content.[1−4] These organics stem from a variety of sources, both anthropogenic and biogenic, resulting in a diverse and complex organic surface composition. In this work, the effect of introducing a surfactant with a very different hydrophobic structure (an aromatic ring) on the stability and morphology of a stearic acid film is explored. Experiments using Langmuir trough methods as well as the *in situ* surface-sensitive spectroscopic technique IRRAS (infrared reflection–absorption spectroscopy) are complemented by molecular dynamics simulations to investigate mixed films of oxidized aromatics (benzoic acid, benzaldehyde) with stearic acid.

Since it is experimentally difficult to probe environmental surfaces directly, two-dimensional model surfaces (such as those provided by the Langmuir trough) are often utilized in laboratory settings. Much work has been performed studying long-chain fatty acid films at the water–air interface, using both pure and multicomponent monolayers.[5−12] Among the common long-chain fatty acids studied are stearic, palmitic, and oleic acids, with similar hydrophobic structure composed of long hydrocarbon chains. These three surfactants in particular are also common surfactants found on the surface of atmospheric aerosols in field studies,[3,4,13,14] primarily due to biogenic emissions. Stearic acid (the fatty acid used in this work) is a well-characterized surfactant, known to produce very stable floating monolayers on water.[7] It exhibits characteristic two-dimensional phase changes at the water surface, finally resulting in collapse[15−18] (fracture of the two-dimensional surface film causing the formation of three-dimensional structures) above pressures of 55 mN/m.[19] This behavior allows for control and monitoring of the morphology and phase behavior of the stearic acid film in a laboratory setting.

In addition to biogenic emissions, environmentally catastrophic events such as the Deepwater Horizon Oil Spill in the Gulf of Mexico in 2010 result in further complicated emissions into the atmosphere, with poorly understood consequences. A NOAA mission collected aerosols in a variety of locations around the spill and discovered that not only was there a higher concentration of volatile organics that had directly evaporated

Special Issue: Ron Naaman Festschrift

Received: March 19, 2013
Revised: June 6, 2013
Published: June 7, 2013

   dx.doi.org/10.1021/jp402737n | J. Phys. Chem. C 2013, 117, 22341−22350

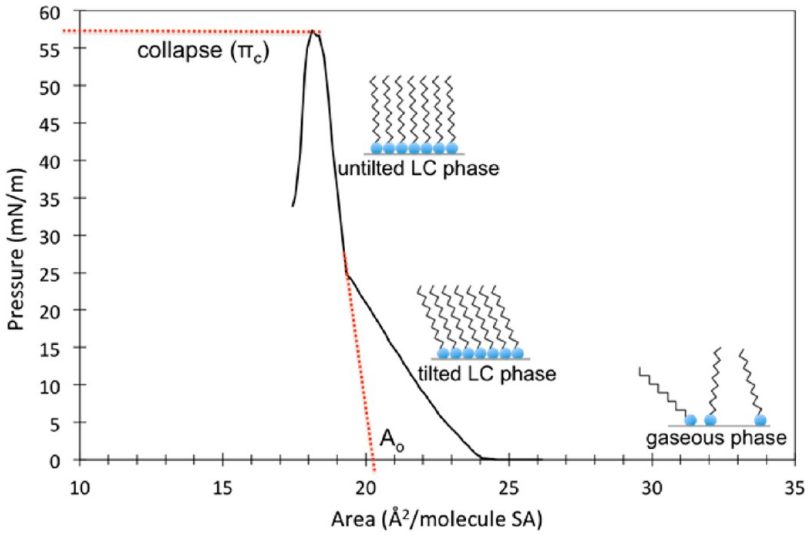

Figure 1. π–A isotherm of a stearic acid (SA) monolayer on water with phase changes labeled (along with schematic representation). The mean molecular area, or footprint (A_o), and collapse pressure (π_c) are also labeled accordingly.

from the oil but also a significant concentration of less-volatile organics.[20,21] Such anthropogenic emissions are then suggested to not only be present in the atmosphere due to catastrophic events such as oil spills but may also be a normal component in other polluted regions of the atmosphere.[20]

Oil, although vastly diverse in composition, can contain a significant concentration of aromatic species.[22] These aromatics differ significantly in hydrophobic structure from biogenic surfactants (e.g., stearic, palmitic, oleic acids) currently taken into consideration in aerosol models and laboratory studies. Although crude oil contains primarily nonpolar (unoxygenated) molecules, once exposed to the atmosphere, they can be readily oxidized.[9,23−27] It has recently been suggested that current field studies of oil spill emissions may be missing a significant fraction of the crude oil released into the environment due to the limitations of their instrumentation which only detect unoxygenated components.[23] Once the oil has been "weathered", a significant fraction contains oxygenated residues, resulting in oxidized surfactants likely to interact at the water surface differently than their unoxidized counterparts.[28] This has further implications on the interactions of oil components with biogenic surfactants naturally present in the atmosphere at the water surface (e.g., the surface of atmospheric aerosols). In this work, we demonstrate the modification to the aqueous surface containing a common biogenic surfactant (stearic acid) due to the presence of two different oxidized aromatics, benzoic acid and benzaldehyde, suggesting the importance of not only the hydrophobic aromatic group but also the identity of the polar group in the mechanism by which the surface is modified.

Finally, the surface morphology of atmospheric aerosol particles has wide-ranging effects on the particle's impact on climate.[27,29−37] Various morphologies have been observed in laboratory studies and in field observations ranging from an inverted micelle structure with the organic components partitioning to the exterior of the particle in a core−shell structure[6,27,38,39] to more complex morphologies containing organic inclusions[40−42] or even surfactant lenses.[43] Two-dimensional films composed of long-chain surfactants (like stearic acid) are known to impede water transfer,[6,44−47] although the quantitative effect on three-dimensional aerosol particles has thus far yielded conflicting results,[10,13,34,48−50] possibly due to these varying surface morphologies. Since aerosol optical properties are dependent upon their size,[51] the ability for the uptake or evaporation of water across the particle surface is an important property to understand. Although compressed single-component monolayers composed of long-chain surfactants will impede water transfer, less work has been performed exploring the more environmentally relevant mixed films with varying hydrophobic character. This work illustrates the complexity of a mixed film with differing hydrophobic groups (both aliphatic and aromatic) to contribute to an understanding of the varying morphologies likely present on aqueous aerosols in the atmosphere.

EXPERIMENTAL AND THEORETICAL METHODS

Materials. All solvents and reagents were used without further purification. Stearic acid (octadecanoic acid, 98+%) was purchased from Aldrich Chemical Co., Inc., and then dissolved in chloroform (ACS grade, Mallinckrodt Baker, Inc.) to a concentration of 1 mg/mL. Benzoic acid (ACS grade, ≥99.5%) was purchased from Sigma-Aldrich and was dissolved to a final concentration of 0.01 M in distilled water. Benzaldehyde (ReagentPlus, ≥99%) was also purchased from Sigma-Aldrich and was prepared to a concentration of 0.01 M in distilled water for the isotherm experiments and to a concentration of 0.002 M for the IRRAS experiment. The higher concentration of 0.01 M could not be used for the IRRAS experiment due to the interference of the gas-phase benzaldehyde signal with the much weaker IRRAS absorbance (the vapor pressure of benzaldehyde is approximately 1 mmHg at 25 °C compared to benzoic acid's 0.001 mmHg at the same temperature). The features in the isotherms with the two different concentrations are similar; however, the extent of modification to the stearic acid film is exacerbated at the lower concentration (see Figure S3, Supporting Information). This difference is attributed to fewer benzaldehyde molecules partitioning into the gas phase during the compression of the surface layer.

Instruments. *Langmuir Trough.* The Langmuir trough for isotherm studies was custom-built, and consists of a PTFE trough (52 × 7 × 0.5 cm^3) coupled to two mechanical, computer-controlled PTFE barriers. These barriers were manipulated using software and a computer interface purchased

dx.doi.org/10.1021/jp402737n | J. Phys. Chem. C 2013, 117, 22341−22350

from KSV-NIMA (Biolin Scientific, Finland). The Langmuir troughs used for both isotherm and IRRAS studies were equipped with a Wilhelmy balance that allowed for the measurement of surface pressure concurrent with the mechanical limitation of the surface area (due to the motion of the barriers across the aqueous surface). The measured surface area is the area between the moving mechanical barriers measured in cm^2, and converted to $Å^2$ $molecule^{-1}$ when stearic acid is present. This produces a surface pressure−area (π−A) isotherm (see Figure 1 for the isotherm of stearic acid), thereby giving interfacial thermodynamic information. In the experiments presented here, isotherm compression/expansion cycles were performed, during which the mechanical barriers continuously moved from their open to closed positions with constant forward and backward barrier speeds (100 cm^2/min) with no wait time between cycles. It should be noted that only the compression isotherms are presented in the isotherm cycle figures in this work.

Infrared Reflection−Absorption Spectroscopy. IRRAS spectra were taken with the external port of a Bruker Tensor 27 FTIR Spectrometer coupled to a NIMA PTFE Langmuir trough (14.5 × 7 × 0.5 cm) controlled using software purchased from KSV-NIMA (Biolin Scientific, Finland). The infrared beam (unpolarized) exited the spectrometer and was passed through a CaF_2 lens before being directed onto the aqueous surface of the Langmuir trough. Two 2 in. diameter gold mirrors were used to direct the IR beam onto the surface, with an angle of incidence of 22° relative to the surface normal, and then to direct the reflected light to the liquid-nitrogen-cooled MCT detector. All optics and equipment (including the Langmuir trough) were constantly purged with dry house air during all experiments. Single channel spectra were collected with a 1 cm^{-1} resolution and were averaged over 200 scans. A single channel spectrum of a bare water surface was used as the background spectrum for the IRRAS spectra collected here. All single channel spectra were atmosphere corrected (compensating for water vapor and CO_2 signals). The resulting reflectance−absorbance (RA) spectrum presented is then obtained using the equation $RA = -\log(R/R_o)$, where R is the IR reflectivity of the surface of interest (in this work, the mixed film of stearic acid and either aqueous benzoic acid or benzaldehyde) and R_o is the IR reflectivity of the bare water surface background. These reflectivities are fully described in the literature using the Fresnel equations, which are presented elsewhere.[52,53] In this experiment, the expected absorption bands will be negative, resulting from the use of unpolarized light incident at an angle of 22° relative to the surface normal of an air−aqueous interface.

Methods. *Isotherm Cycles.* Aqueous solutions of benzaldehyde or benzoic acid were prepared to the concentrations specified above, and spread on the corresponding Langmuir trough. The stearic acid solution (1 mg/mL in chloroform) was immediately spread on the aqueous interface (10 μL for the IRRAS experiment and 30 μL for the isotherm cycles only), and the solvent was allowed to evaporate for 20 min without any disruption. After solvent evaporation, isotherm compression−expansion cycles were performed (the pressure was zeroed immediately prior to the start of the cycles to result in all surface pressure readings being relative to the initial surface conditions), with the mechanical trough barriers progressing at a constant speed between their fully open position (280 cm^2 for the large trough for isotherm measurements and 70 cm^2 for the small trough used in the IRRAS measurements) and a maximum surface pressure of 40 mN/m (remaining well below the collapse pressure, π_c, indicated in Figure 1, of the stearic acid film). IRRAS spectra were taken with the barriers fully open (surface area of 70 cm^2) before isotherm cycles for both aromatics, after three isotherm cycles for benzaldehyde, and after four isotherm cycles for benzoic acid.

Molecular Dynamics Simulations. The stearic acid and aromatic compound interaction parameters were obtained using the automated topology builder (ATB) and repository.[54] Two stearic acid films were initially composed of 196 stearic molecules each, arranged in such a way as to yield an area of 21 $Å^2$ $molecule^{-1}$. The stearic acid molecules were assembled in two rectangular arrays with 14 × 14 molecules each in the x and y directions, respectively, separated by 6 nm in the z-axis with the polar heads pointing to the aqueous phase. The space between the two stearic acid films was filled with 20 molecules of aromatic compounds and ∼8000 SPC water molecules[55] at random positions, and the box edge along the z direction was set to 50 nm, resulting in one stearic film on each air−aqueous solution interface. Aqueous solutions of benzaldehyde and benzoic acid were also built inside a box with the same dimensions, resulting in two air−aqueous solution interfaces without the stearic acid film. The periodic boundary conditions produce an infinite slab with two air−aqueous solution interfaces perpendicular to the z-axis at a constant volume. Twenty molecules of aromatic compounds and ∼8000 SPC water molecules were randomly generated within a slab of 6 nm in the middle of this box of 50 nm in the z direction, yielding approximately 0.15 mol L^{-1} aqueous solutions of aromatic compounds. The lower concentration of 0.01 M could not be used in the MD simulation due to the need of about 10 times more water molecules, which is unfeasible computationally. On the other hand, only two molecules of aromatic compounds with ∼8000 SPC water molecules yield a concentration of 0.01 M, but in this system, it would be impossible to visualize the aggregates inside the ensemble as we desire to observe in the MD simulation.

These structures were equilibrated using 5000 steps of the steepest descent, followed by L-BFGS minimization[56,57] to avoid strong repulsive contacts between stearic acid molecules. Then, a molecular dynamics simulation was used to relax the system for 200 ps. Finally, a 50 ns molecular dynamics simulation was performed to estimate the thermodynamic properties of the system using the constant number of particles N, volume V, and temperature T (NVT) ensemble. This last step was performed using weak thermal coupling (τ_T = 0.1 ps) at T = 298 K.[58]

Trajectories were run up to 50 ns with a time step of 2 fs without any geometry constraint. Nonbonded interactions were truncated using a 1.0 and 1.2 nm twin-range cutoff for Lennard-Jones and Coulomb interactions, respectively. Dispersion correction was applied to the energy, and the neighbor list was updated every 10 steps. All analyses were performed using the last 30 ns of the data for mass density and order parameter of the film, using coordinates and energies recorded at 2 ps intervals. All simulations were carried out using the GROMACS 4.5.3 package.[59]

Besides characterizing which orientation corresponds to each isotherm, molecular dynamics simulations allow a thorough description of the molecular organization for each film. This is an important issue because the degree of order may be correlated with the order parameter (S_z), which is related to the average spatial orientation of molecules and may be defined as

dx.doi.org/10.1021/jp402737n | J. Phys. Chem. C 2013, 117, 22341−22350

$$S_z = \frac{1}{2}\langle 3\cos^2\theta_z - 1\rangle$$

where θ_z is the angle between a reference vector in stearic acid molecules and the z-axis and the brackets denote the average over all equivalent atoms and over time. From MD simulations, the order parameter is calculated for consecutive C−C bonds. As a united atom force field is used (without hydrogen or deuterium atoms), the C−D bond vector needs to be reconstructed. To do so, the C(i − 1)−C(i + 1) vector for each i C atom is usually taken to be the z-axis. The x- and y-axes are defined perpendicular to the z-axis and to each other, with the y-axis in the C(i − 1)−C(i)−C(i + 1) plane. Using this definition, S_z can be compared bond by bond directly to 2H-NMR data. The perpendicular direction emerges as a natural choice to compute order parameters for monolayers spread on the x−y plane. S_z values range from −0.5 to +1.0, meaning an orientation either fully perpendicular or fully parallel to the z-axis, respectively. A value of around 0 means an average random orientation of the vector with respect to the z-axis. For the aliphatic atoms, the line joining the reference atom and the next heavy atom attached to it will define the vectors.

RESULTS

In this work, mixed films of oxidized aromatics (benzaldehyde and benzoic acid) with a well-known aliphatic compound (stearic acid) are explored experimentally using Langmuir trough methods and infrared reflection−absorption spectroscopy (IRRAS), and theoretically using molecular dynamics (MD) simulations. The phase changes of surfactant films at the water surface are described in detail elsewhere,[60−63] but those of stearic acid will be briefly summarized here with reference to the depiction in Figure 1. Two-dimensional phase changes are indicated in the π−A isotherm by sharp slope changes (discontinuities, e.g., kinks or plateaus). In a stearic acid isotherm (Figure 1), the film begins (moving from large to small area, right to left on the area axis) in a disordered two-dimensional gaseous phase where the molecules are highly fluid and disordered on the surface (negligible surface pressure). Then, in stearic acid, the film transitions directly to a tilted liquid condensed phase,[64,65] where the molecules are ordered but tilted relative to the interface.[63] Finally, the stearic acid molecules transition to an untilted liquid condensed phase where the molecules are tightly packed and occupy a minimum area at the surface.

Conventionally, the untilted liquid condensed phase is extrapolated to zero surface pressure, yielding a characteristic area that the molecule occupies at the surface, or its "footprint" (A_o, Figure 1). For stearic acid, the footprint is known to be ca. 20 Å^2 molecule^{-1}.[7] The footprint of a surfactant is a useful tool for following modifications to the surface morphology and/or composition. When isotherm compression−expansion cycles were performed for a pure stearic acid monolayer, this footprint changed by less than 1 Å^2 molecule^{-1}, illustrating the stability and reproducibility of the phases exhibited by a floating stearic acid film.[66] However, in the same work, when phenylalanine was also present in the surface region, significant disruption of the stearic acid film was observed in the isotherm cycles, evidenced by the significant loss of the stearic acid character from the isotherms seen in the decrease of its footprint over the course of the isotherm cycles.[66] In addition to the decrease in footprint, there was also a decrease in slope of the untilted liquid condensed phase, indicating a decline in phase stability.

In this work, a similar analysis can be employed utilizing a stearic acid film deposited on an aqueous solution of benzoic acid or benzaldehyde, two decreasingly oxidized aromatics (isotherm cycles shown in Figure 2a and b, respectively). Both

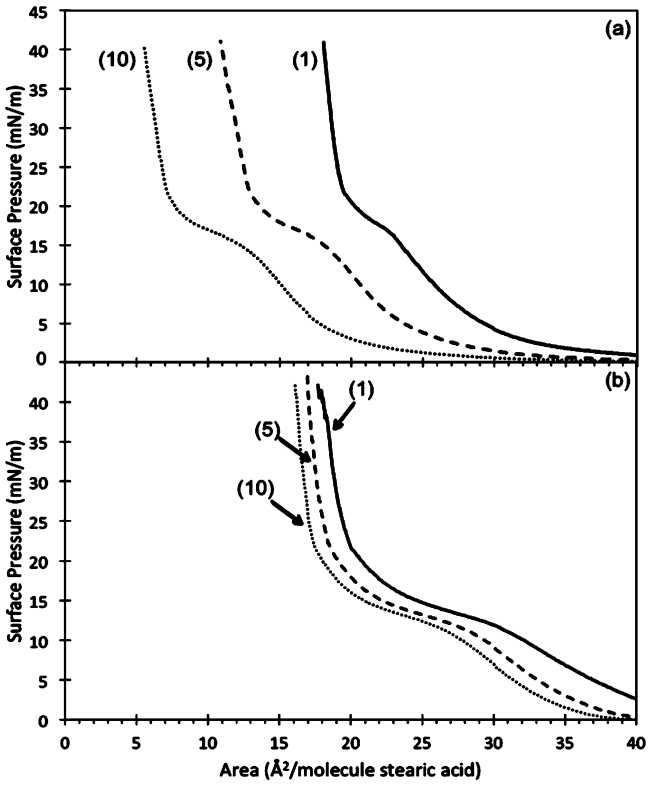

Figure 2. Aromatic−stearic acid mixed film π−A isotherm cycles. Only compression isotherms from cycles 1, 5, and 10 are shown (as indicated). (a) Benzoic acid (0.01 M)−stearic acid mixed film. (b) Benzaldehyde (0.01 M)−stearic acid mixed film.

benzoic acid and benzaldehyde are surface active, exhibiting an increased surface pressure at small surface areas in both pure aqueous solution isotherms (see Figure S1, Supporting Information) as well as in MD simulations of the pure aqueous solutions in the absence of stearic acid (Figure S2, Supporting Information). This is consistent with previous MD simulations performed on aqueous solutions of anionic benzoate as well as other aromatics, which indicated the strong surface propensity of these molecules.[67] In the mixed film of benzoic acid and stearic acid (Figure 2a), the isotherm plateaus around 16 mN/m, the same surface pressure the isotherm of pure aqueous benzoic acid changes slope (Figure S1, Supporting Information). Therefore, this feature is due to the presence of benzoic acid. Analogously, in Figure 2b, the plateau around 12.5 mN/m is due to benzaldehyde, with the same surface pressure exhibiting a phase change in the pure benzaldehyde isotherm (Figure S1, Supporting Information). After these plateaus, there is a sharp increase in surface pressure due to the phase change in stearic acid to its untilted liquid condensed phase. Analogously to the pure stearic acid isotherm, this phase may be extrapolated to zero surface pressure to yield the footprint of stearic acid. In both parts a and b of Figure 2 in isotherm cycle 1, the stearic acid footprint is comparable to its value in its pure monolayer (ca. 20 Å^2 molecule^{-1}). Then, as the isotherm cycles progress, the benzoic acid−stearic acid mixed film (Figure 2a) exhibits a marked decrease in the stearic acid footprint,

dx.doi.org/10.1021/jp402737n | J. Phys. Chem. C 2013, 117, 22341−22350

indicating modification to the stearic acid film due to the presence of benzoic acid, while the decrease in the stearic acid footprint in the benzaldehyde–stearic acid mixed film (Figure 2b) is less pronounced, indicating a lesser modification.

The IRRAS spectra in Figure 3 yield further insight into the modification of the stearic acid film due to the aromatic group

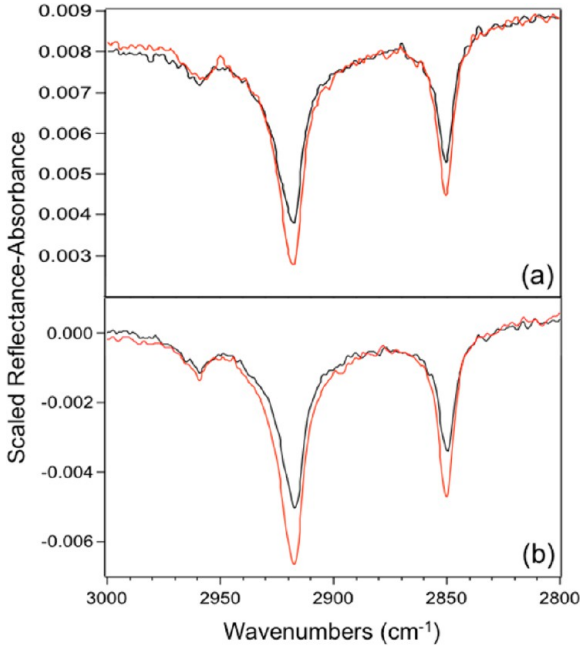

Figure 3. IRRAS spectra before isotherm cycles (black) and after isotherm cycles (red) for (a) benzoic acid (0.01 M)–stearic acid mixed film and (b) benzaldehyde (0.002 M)–stearic acid mixed film.

present on both benzaldehyde and benzoic acid. The most prominent peaks at 2918 and 2850 cm^{-1} are due to the asymmetric and symmetric CH_2 stretches, respectively, of the stearic acid molecules present at the surface. The C–H stretching region in IRRAS spectra is sensitive to orientational ordering changes at the surface.[68,69] Here, there is an increase in intensity in the C–H stretch region in both the stearic acid–benzaldehyde and stearic acid–benzoic acid mixed films after the films have been subjected to a few isotherm compression–expansion cycles. As has been noted in phospholipid monolayers, this can be indicative of either more molecules in the illuminated surface area or a change in the orientational ordering of the hydrocarbon tails of the surface molecules.[68] Both of these cases can indicate a prematurely condensed stearic acid film at the surface.

This claim is supported by the calculated order parameters and tilt angles of pure stearic acid versus the mixed aromatic–stearic acid films. In the study of molecular monolayers with large hydrocarbon chains, it is useful to characterize the relative order of these chains with respect to a reference axis. Experimentally, the deuterium order parameter is obtained by NMR, where the hydrocarbon chains are selectively deuterated and the resultant angle between the deuterium and carbon backbone is measured relative to an axis perpendicular to the interface. Figure 4 shows the calculated deuterium order parameters for pure stearic acid (red circles), mixed benzaldehyde/stearic acid (black squares), and mixed benzoic acid/stearic acid (green triangles) films. Our MD simulations show that mixed benzaldehyde/stearic acid films and mixed

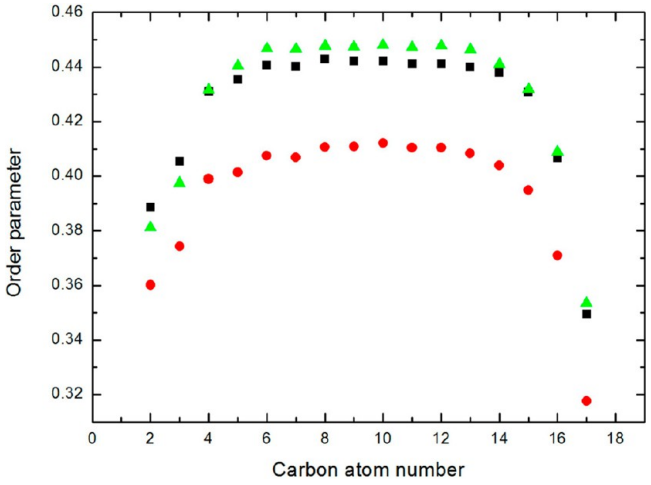

Figure 4. The deuterium order parameters for pure stearic acid (red circles), mixed benzaldehyde/stearic acid film (black squares), and mixed benzoic acid/stearic acid film (green triangles) at the interface after 50 ns at 21 $Å^2$ $molecule^{-1}$.

benzoic acid/stearic acid films are slightly more ordered than the pure stearic acid film. This result is consistent with all carbon atoms in the hydrocarbon chain. Further, the calculated tilt angle (θ) of the pure stearic acid film relative to the stearic acid film mixed with benzaldehyde/benzoic is around 20°, which is the angular shift caused by the formation of benzaldehyde or benzoic acid aggregates. It is important to note that the stearic acid film mixed with benzaldehyde or benzoic aggregates is more perpendicular to the interface than the pure stearic acid film because of the increase of packing caused by the inclusion of benzaldehyde or benzoic acid molecules into the stearic acid film, i.e., less room available among stearic acid molecules. In both the IRRAS spectra (Figure 3) as well as the calculated order parameters (Figure 4) and tilt angles, the presence of benzaldehyde or benzoic acid is shown to reduce the area available for the stearic acid molecules, which facilitates their alignment with the normal axis with respect to the interface.

Snapshots of the MD simulations performed are shown in Figures 5–7. Figure 5 portrays the benzoic acid/stearic acid system during the first 7 ns of the simulation (the total simulation time was 50 ns). At the beginning of the simulation, the benzoic acid molecules are distributed throughout the bulk solution (0 ns) but partition to the interfacial region within the first 7 ns of simulation. Figure 5 also illustrates the propensity of these aromatic molecules to form aggregates through π-stacking of the aromatic rings. Benzaldehyde exhibited similar behavior and is therefore not shown explicitly here. The simulations were allowed to proceed for a total of 50 ns, after which snapshots were taken and are presented in Figures 6 (stearic acid only, benzaldehyde/stearic acid mixed film) and 7 (benzoic acid/stearic acid mixed film). In Figure 6, the resulting mixed film of benzaldehyde and stearic acid is shown in parts A (front view) and B (view from the bulk toward the interface), with stearic acid only presented in parts C (front view) and D (view from the bulk toward the interface) for comparison. First, stearic acid remains as an ordered stable film after 50 ns of simulation. Looking from the bulk at the interface (Figure 6D), there is a fairly uniform coverage of stearic acid molecules, in a sense shielding the bulk phase from the air above the film. In the benzaldehyde/stearic acid mixed film, however, the

dx.doi.org/10.1021/jp402737n | J. Phys. Chem. C 2013, 117, 22341–22350

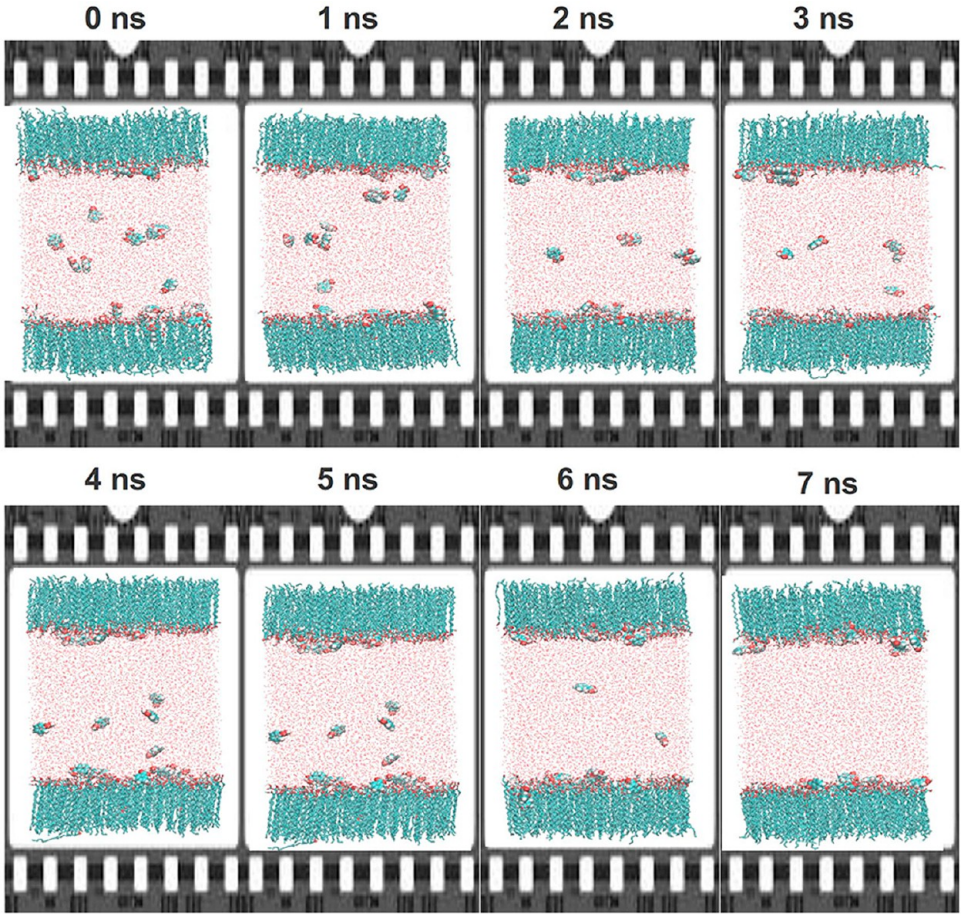

Figure 5. Sample snapshots of the first 7 ns of benzoic acid adsorption at the interfacial region. During this time, the benzoic acid molecules are seen to migrate to the interface and into the hydrocarbon chains, forming π-stacked aggregates.

benzaldehyde molecules are seen to have intercalated into the stearic acid film (Figure 6A), forming π-stacked aggregates within the hydrocarbon chains of the stearic acid film layer. Figure 7 then shows the benzoic acid/stearic acid mixed film after 50 ns, again from both a front view (Figure 7A) and viewed from the bulk toward the interface (Figure 7B). As with benzaldehyde in Figure 6, benzoic acid intercalates into the stearic acid film. However, rather than retaining its π-stacked aggregate form, it forms dimers within the stearic acid film through hydrogen bonding of the carboxylic acid head groups following the orientation of the hydrocarbon chains of the stearic acid film. The result of both of these aromatic molecules intercalating into the stearic acid film is a perturbation to the ordered film layer, forming "holes" or regions lacking in surfactant coverage (region circled in Figures 6B and 7B). These "holes" allow for easier access to bulk molecules, regardless of the compressed state of the surfactant film. These aggregates (both the π-stacked aggregates of benzaldehyde and the H-bonded aggregates of benzoic acid) are also the source of the tilt angle change of the stearic acid film seen in both the calculated value described above and in the IRRAS spectra shown in Figure 3.

DISCUSSION

This work explores the effect of the interaction of an aromatic soluble surfactant with a stearic acid film. Previously, one aromatic molecule, L-phenylalanine, was seen to interact with the stearic acid monolayer and cause "early hydrophobic collapse" of the aliphatic film.[66] It was then suggested that this collapse was specifically caused by hydrophobic interactions between the aromatic ring of phenylalanine and the hydrocarbon tail of stearic acid. The bulky aromatic ring caused splaying of the otherwise ordered tails of the stearic acid molecules, analogous to the micelle-like clusters named "solitons" by Safran et al.,[70] resulting in the formation of hydrophobic aggregates at the surface. These aggregates were evidenced by diminishing stearic acid character in the isotherm cycles, and were directly visualized using Brewster angle microscopy (BAM). This work expands on the work previously done by exploring the effect of changing the hydrophilic group of the aromatic molecule, while also adding MD simulations to yield a molecular visualization of the stearic acid film disruption.

It is clear from the results due to phenylalanine as well as the aromatic molecules used in this work that the significantly different hydrophobic groups (between stearic acid and the aromatic molecules) present at the surface facilitate the modification to the stearic acid film. However, this work also illustrates the role of the hydrophilic group in this surface modification. The aldehyde group on benzaldehyde, although hydrophilic, is not as oxidized as the carboxylic acid group on benzoic acid. This results in benzoic acid having a higher propensity for hydrogen bonding (as seen in the dimers formed within the surface film seen in Figure 7A) as well as being much less volatile than other aromatics. Benzaldehyde has a lower propensity for hydrogen bonding, and hence a much higher vapor pressure. Both aromatics do intercalate into the stearic

dx.doi.org/10.1021/jp402737n | J. Phys. Chem. C 2013, 117, 22341−22350

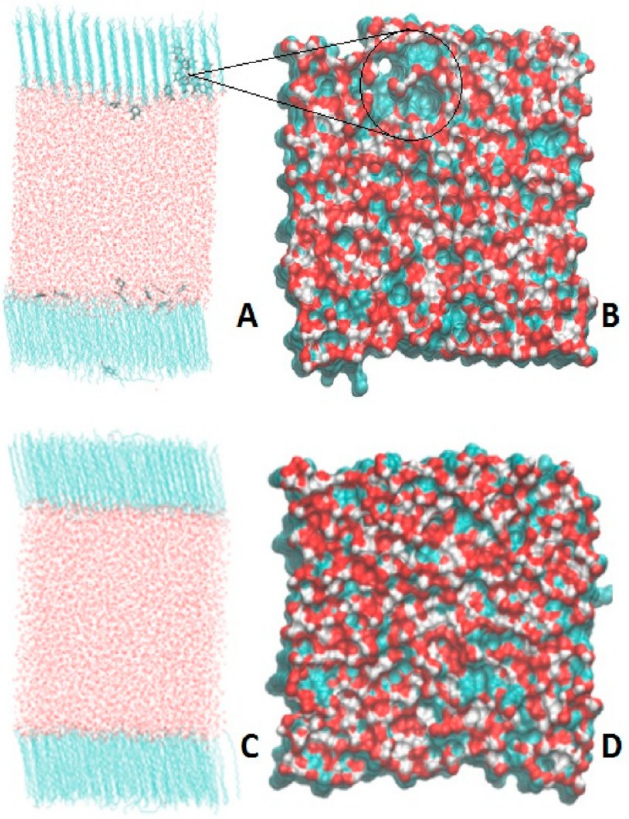

Figure 6. Mixed benzaldehyde/stearic acid film (A and B) and a pure stearic acid film (C and D) at the air−water interface after 50 ns of simulation time with a molecular area of 21 Å^2 per molecule of stearic acid. Parts A and C are from a front view. Parts B and D are from the bulk toward the top layer. The "holes" appear in the mixed film (B) but not in the pure film (C), i.e., the control system.

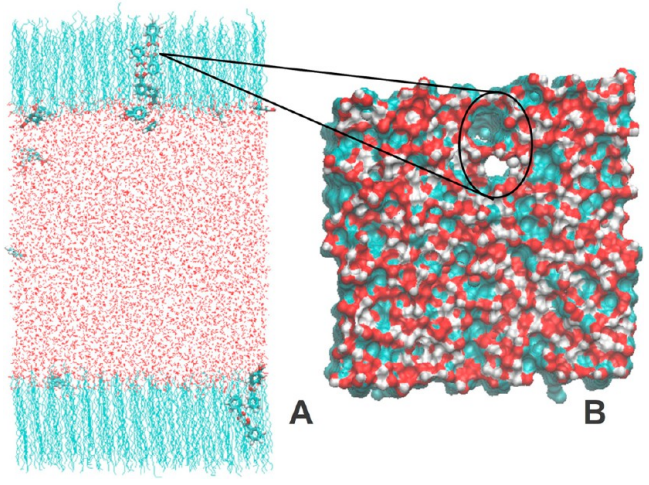

Figure 7. Mixed benzoic acid/stearic acid film at the interface after 50 ns at 21 Å^2 molecule^{-1}. In the front view in (A) aggregation oriented in the direction of the hydrocarbon chains is observed. The view from the bulk toward the top layer is presented in (B), showing "holes" in the film.

acid film, but with increased surface pressure invoked by the mechanical barriers, they behave differently due to their hydrophilic character. Benzaldehyde, with its higher volatility, is easily squeezed out into the gas phase, resulting in very little enduring modification to the stearic acid film throughout the isotherm cycles (Figure 2b) beyond the initial change in orientation of the hydrocarbon tails (evidenced by IRRAS C−H stretch intensity increase and calculated stearic acid tilt angle and order parameters). In contrast, benzoic acid has a much more pronounced disruption of the stearic acid film with repeated isotherm cycles (Figure 2a). Because of its ability to hydrogen bond much more strongly to itself, as seen in Figure 7A, and to the water molecules or stearic acid molecules in the interfacial region, benzoic acid is much less volatile and is retained in the stearic acid film. Rather than being squeezed out into the gas phase as benzaldehyde does, benzoic acid remains in the interfacial layer and forces further, more long-lasting, modification to the stearic acid film with increased external pressure from the mechanical barriers, evidenced by the more significant decrease in stearic acid footprint with isotherm cycles (Figure 2a). Note, however, that, although the footprint of stearic acid decreases, the slope remains consistent. This is in contrast with the complete loss of stability of the stearic acid film evidenced by a significant decrease in slope of the untilted liquid condensed phase seen in the phenylalanine/stearic acid mixed film system.[66] Although both benzoic acid and phenylalanine modify the stearic acid film, their effect is qualitatively different.

The data presented here along with the previous work on the phenylalanine/stearic acid mixed film system[66] yields a more complete picture of the effect of aromatics on aliphatic films. Although the largely different hydrophobic group provided by the aromatic ring does facilitate the adsorption to the interfacial region as well as the initial surface film disruption (orientation and ordering change), the extent of modification with repeated changes in surface pressure (during the isotherm cycles) is greatly affected by the hydrophilic headgroup. Although a detailed mechanism has yet to be obtained, this work indicates that there is a complex interplay between the hydrophilic headgroup as well as the hydrophobic group in facilitating the modification to the surfactant film. It is clear that the aromatic hydrophobic group drives the surface adsorption as well as mediates aggregate formation through π-stacking (at least initially, although the aggregate structure may change at later times, as evidenced in the benzoic acid case here). These aggregates initially alter the orientation of the surfactant hydrocarbon chains (see IRRAS spectra in Figure 3 as well as calculated order parameters in Figure 4). Any further modification to the stearic acid film however is determined by the nature of the hydrophilic headgroup. Without the ability to strongly hydrogen bond, the aromatics may simply be squeezed out into the gas phase without significant alteration of the surface, as seen in the benzaldehyde case here. With the ability to hydrogen bond, however, the initial π-stacked aggregates may transition to hydrogen-bonded dimers that remain within the surfactant hydrocarbon tails, inducing further surface modification (see isotherm cycles in Figure 2a).

■ ATMOSPHERIC IMPLICATIONS

Understanding the surface morphology of atmospheric aerosol particles is of great importance in determining the particle's effect on climate, due to the surface's impact on water transfer into and out of the particle. Although two-dimensional surface films of long-chain fatty acids are known to impede water transfer, this work illustrates that the presence of a soluble surfactant with a significantly different hydrophobic structure may significantly change the surface morphology, and hence the

dx.doi.org/10.1021/jp402737n | J. Phys. Chem. C 2013, 117, 22341−22350

water transfer properties. Long-chain fatty acids such as stearic acid used here are the primary surfactants found on atmospheric aerosol particles but stem primarily from biogenic sources. Emissions from anthropogenic sources such as oil spills can significantly alter the composition of the aerosol particles, with oil components existing in a variety of oxygenated states after atmospheric weathering. The oxidized aromatic components from these emissions can greatly complicate the surface morphology of aerosol particles containing some portion of a biogenic surfactant coating, forcing regions of the aerosol core to be exposed despite the surfactant coating. This destabilization of the surface film is expected to induce greater permeability of the particle as a whole to water, thereby changing the size of the particle and hence its impact on climate.

■ ASSOCIATED CONTENT

Ⓢ Supporting Information

π−A isotherms of aqueous benzoic acid and benzaldehyde are provided in the absence of stearic acid, as well as their corresponding MD simulations. Also, π−A isotherms of the benzaldehyde−stearic acid mixed film system under the conditions described for the IRRAS spectra are provided. This material is available free of charge via the Internet at http://pubs.acs.org.

■ AUTHOR INFORMATION

Corresponding Author

*Phone: 303-492-8605. E-mail: vaida@colorado.edu.

Notes

The authors declare no competing financial interest.

■ ACKNOWLEDGMENTS

V.V. and E.C.G. acknowledge support for this work from the National Science Foundation (CHE 1011770). E.C.G. also acknowledges support from a NASA Earth and Space Science Graduate Fellowship as well as a Marian Sharrah Graduate Fellowship. A.S.P. acknowledges the CNPq funding (481481/2010-9) and the FAPERJ YoungScientist award (E-26/101.452/2010). T.R.C.G. acknowledges a CAPES PNPD postdoc fellowship (02559/09-9). G.S.T. acknowledges that NCAR is operated by the University Corporation for Atmospheric Research under sponsorship from the US National Science Foundation.

■ REFERENCES

(1) Jimenez, J. L.; Canagaratna, M. R.; Donahue, N. M.; Prevot, A. S. H.; Zhang, Q.; Kroll, J. H.; DeCarlo, P. F.; Allan, J. D.; Coe, H.; Ng, N. L.; et al. Evolution of Organic Aerosols in the Atmosphere. *Science* **2009**, *326* (5959), 1525−1529.

(2) McNeill, V. F.; Sareen, N.; Schwier, A. *Surface-Active Organics in Atmospheric Aerosols*; Springer: Berlin, Heidelberg, 2013; pp 1−59.

(3) Tervahattu, H.; Hartonen, K.; Kerminen, V. M.; Kupiainen, K.; Aarnio, P.; Koskentalo, T.; Tuck, A. F.; Vaida, V. New Evidence of an Organic Layer on Marine Aerosols. *J. Geophys. Res.: Atmos.* **2002**, *107* (D7−8).

(4) Tervahattu, H.; Juhanoja, J.; Vaida, V.; Tuck, A. F.; Niemi, J. V.; Kupiainen, K.; Kulmala, M.; Vehkamaki, H. Fatty Acids on Continental Sulfate Aerosol Particles. *J. Geophys. Res.: Atmos.* **2005**, *110* (D6), 9.

(5) Gilman, J. B.; Tervahattu, H.; Vaida, V. Interfacial Properties of Mixed Films of Long-Chain Organics at the Air-Water Interface. *Atmos. Environ.* **2006**, *40* (34), 6606−6614.

(6) Donaldson, D. J.; Vaida, V. The Influence of Organic Films at the Air-Aqueous Boundary on Atmospheric Processes. *Chem. Rev.* **2006**, *106* (4), 1445−1461.

(7) Gilman, J. B.; Eliason, T. L.; Fast, A.; Vaida, V. Selectivity and Stability of Organic Films at the Air-Aqueous Interface. *J. Colloid Interface Sci.* **2004**, *280* (1), 234−243.

(8) Ocko, B. M.; Kelley, M. S.; Nikova, A. T.; Schwartz, D. K. Structure and Phase Behavior of Mixed Monolayers of Saturated and Unsaturated Fatty Acids. *Langmuir* **2002**, *18* (25), 9810−9815.

(9) Mmereki, B. T.; Donaldson, D. J.; Gilman, J. B.; Eliason, T. L.; Vaida, V. Kinetics and Products of the Reaction of Gas-Phase Ozone with Anthracene Adsorbed at the Air-Aqueous Interface. *Atmos. Environ.* **2004**, *38* (36), 6091−6103.

(10) Gilman, J. B.; Vaida, V. Permeability of Acetic Acid through Organic Films at the Air-Aqueous Interface. *J. Phys. Chem. A* **2006**, *110* (24), 7581−7587.

(11) Rontu, N.; Vaida, V. Surface Partitioning and Stability of Pure and Mixed Films of 8−2 Fluorotelomer Alcohol at the Air-Water Interface. *J. Phys. Chem. C* **2007**, *111* (31), 11612−11618.

(12) Rontu, N.; Vaida, V. Miscibility of Perfluorododecanoic Acid with Organic Acids at the Air-Water Interface. *J. Phys. Chem. C* **2007**, *111* (27), 9975−9980.

(13) Giddings, W. P.; Baker, M. B. Sources and Effects of Monolayers on Atmospheric Water Droplets. *J. Atmos. Sci.* **1977**, *34* (12), 1957−1964.

(14) Tervahattu, H.; Juhanoja, J.; Kupiainen, K., Identification of an Organic Coating on Marine Aerosol Particles by Tof-Sims. *J. Geophys. Res.: Atmos.* **2002**, *107* (D16).

(15) Ybert, C.; Lu, W.; Möller, G.; Knobler, C. M. Collapse of a Monolayer by Three Mechanisms. *J. Phys. Chem. B* **2002**, *106* (8), 2004−2008.

(16) Vollhardt, D. Nucleation in Monolayers. *Adv. Colloid Interface Sci.* **2006**, *123*−*126*, 173−188.

(17) Angelova, A.; Vollhardt, D.; Ionov, R. 2d-3d Transformations of Amphiphilic Monolayers Influenced by Intermolecular Interactions: A Brewster Angle Microscopy Study. *J. Phys. Chem.* **1996**, *100* (25), 10710−10720.

(18) Smith, R. D.; Berg, J. C. Collapse of Surfactant Monolayers at the Air-Water Interface. *J. Colloid Interface Sci.* **1980**, *74* (1), 273−286.

(19) Roberts, G. *Langmuir-Blodgett Films*; Plenum Press: New York, 1990.

(20) de Gouw, J. A.; Middlebrook, A. M.; Warneke, C.; Ahmadov, R.; Atlas, E. L.; Bahreini, R.; Blake, D. R.; Brock, C. A.; Brioude, J.; Fahey, D. W.; et al. Organic Aerosol Formation Downwind from the Deepwater Horizon Oil Spill. *Science* **2011**, *331* (6022), 1295−1299.

(21) Bahreini, R.; Middlebrook, A. M.; Brock, C. A.; de Gouw, J. A.; McKeen, S. A.; Williams, L. R.; Daumit, K. E.; Lambe, A. T.; Massoli, P.; Canagaratna, M. R.; et al. Mass Spectral Analysis of Organic Aerosol Formed Downwind of the Deepwater Horizon Oil Spill: Field Studies and Laboratory Confirmations. *Environ. Sci. Technol.* **2012**, *46* (15), 8025−8034.

(22) Coleman, J.; Baker, J.; Cooper, C.; Fingas, M.; Hunt, G.; Kvenvolden, K.; Michel, K.; Michel, J.; McDowell, J.; Phinney, J.; et al. *Oil in the Sea III: Inputs, Fates, and Effects*; The National Academies Press: 2003.

(23) Aeppli, C.; Carmichael, C. A.; Nelson, R. K.; Lemkau, K. L.; Graham, W. M.; Redmond, M. C.; Valentine, D. L.; Reddy, C. M. Oil Weathering after the Deepwater Horizon Disaster Led to the Formation of Oxygenated Residues. *Environ. Sci. Technol.* **2012**, *46* (16), 8799−8807.

(24) Garrett, R. M.; Pickering, I. J.; Haith, C. E.; Prince, R. C. Photooxidation of Crude Oils. *Environ. Sci. Technol.* **1998**, *32* (23), 3719−3723.

(25) Eliason, T. L.; Aloisio, S.; Donaldson, D. J.; Cziczo, D. J.; Vaida, V. Processing of Unsaturated Organic Acid Films and Aerosols by Ozone. *Atmos. Environ.* **2003**, *37*, 2207−2219.

(26) Eliason, T. L.; Gilman, J. B.; Vaida, V. Oxidation of Organic Films Reevant to Atmospheric Aerosols. *Atmos. Environ.* **2004**, *38*, 1367−1378.

(27) Ellison, G. B.; Tuck, A. F.; Vaida, V. Atmospheric Processing of Organic Aerosols. *J. Geophys. Res.* **1999**, *104* (D9), 11,633−11,641.
(28) Khabiri, M.; Roeselova, M.; Cwiklik, L. Properties of Oxidized Phospholipid Monolayers: An Atomistic Molecular Dynamics Study. *Chem. Phys. Lett.* **2012**, *519*−*20*, 93−99.
(29) Lang-Yona, N.; Abo-Riziq, A.; Erlick, C.; Segre, E.; Trainic, M.; Rudich, Y. Interaction of Internally Mixed Aerosols with Light. *Phys. Chem. Chem. Phys.* **2010**, *12* (1), 21−31.
(30) Riziq, A. A.; Trainic, M.; Erlick, C.; Segre, E.; Rudich, Y. Extinction Efficiencies of Coated Absorbing Aerosols Measured by Cavity Ring Down Aerosol Spectrometry. *Atmos. Chem. Phys.* **2008**, *8* (6), 1823−1833.
(31) Kwamena, N. O. A.; Buajarern, J.; Reid, J. P. Equilibrium Morphology of Mixed Organic/Inorganic/Aqueous Aerosol Droplets: Investigating the Effect of Relative Humidity and Surfactants. *J. Phys. Chem. A* **2010**, *114* (18), 5787−5795.
(32) Hearn, J. D.; Smith, G. D. Measuring Rates of Reaction in Supercooled Organic Particles with Implications for Atmospheric Aerosol. *Phys. Chem. Chem. Phys.* **2005**, *7* (13), 2549−2551.
(33) Fuzzi, S.; Andreae, M. O.; Huebert, B. J.; Kulmala, M.; Bond, T. C.; Boy, M.; Doherty, S. J.; Guenther, A.; Kanakidou, M.; Kawamura, K.; et al. Critical Assessment of the Current State of Scientific Knowledge, Terminology, and Research Needs Concerning the Role of Organic Aerosols in the Atmosphere, Climate, and Global Change. *Atmos. Chem. Phys.* **2006**, *6*, 2017−2038.
(34) Garland, R. M.; Wise, M. E.; Beaver, M. R.; DeWitt, H. L.; Aiken, A. C.; Jimenez, J. L.; Tolbert, M. A. Impact of Palmitic Acid Coating on the Water Uptake and Loss of Ammonium Sulfate Particles. *Atmos. Chem. Phys.* **2005**, *5*, 1951−1961.
(35) Wise, M. E.; Baustian, K. J.; Tolbert, M. A. Internally Mixed Sulfate and Organic Particles as Potential Ice Nuclei in the Tropical Tropopause Region. *Proc. Natl. Acad. Sci. U.S.A.* **2010**, *107* (15), 6693−6698.
(36) Wise, M. E.; Garland, R. M.; Tolbert, M. A.; Ice Nucleation in Internally Mixed Ammonium Sulfate/Dicarboxylic Acid Particles. *J. Geophys. Res.: Atmos.* **2004**, *109*, 19.
(37) Vaida, V.; Tuck, A. F.; Ellison, G. B. Optical and Chemical Properties of Atmospheric Organic Aerosols. *Phys. Chem. Earth, Part C* **2000**, *25* (3), 195−198.
(38) Gill, P. S.; Graedel, T. E.; Weschler, C. J. Organic Films on Atmospheric Aerosol-Particles, Fog Droplets, Cloud Droplets, Raindrops, and Snowflakes. *Rev. Geophys.* **1983**, *21* (4), 903−920.
(39) Wyslouzil, B. E.; Wilemski, G.; Strey, R.; Heath, C. H.; Dieregsweiler, U. Experimental Evidence for Internal Structure in Aqueous - Organic Nanodroplets. *Phys. Chem. Chem. Phys.* **2006**, *8* (1), 54−57.
(40) Kanakidou, M.; Seinfeld, J. H.; Pandis, S. N.; Barnes, I.; Dentener, F. J.; Facchini, M. C.; Van Dingenen, R.; Ervens, B.; Nenes, A.; Nielsen, C. J.; et al. Organic Aerosol and Global Climate Modelling: A Review. *Atmos. Chem. Phys.* **2005**, *5* (4), 1053−1123.
(41) Laurain, A. M. C.; Reid, J. P. Characterizing Internally Mixed Insoluble Organic Inclusions in Aqueous Aerosol Droplets and Their Influence on Light Absorption. *J. Phys. Chem. A* **2009**, *113* (25), 7039−7047.
(42) Rudich, Y.; Donahue, N. M.; Mentel, T. F. Aging of Organic Aerosol: Bridging the Gap between Laboratory and Field Studies. *Annu. Rev. Phys. Chem.* **2007**, *58* (1), 321−352.
(43) Reid, J. P.; Dennis-Smither, B. J.; Kwamena, N. O. A.; Miles, R. E. H.; Hanford, K. L.; Homer, C. J. The Morphology of Aerosol Particles Consisting of Hydrophobic and Hydrophilic Phases: Hydrocarbons, Alcohols and Fatty Acids as the Hydrophobic Component. *Phys. Chem. Chem. Phys.* **2011**, *13* (34), 15559−15572.
(44) Rideal, E. K. The Influence of Thin Surface Films on the Evaporation of Water. *J. Phys. Chem.* **1925**, *29*, 1585−1588.
(45) Langmuir, I.; Schaefer, V. J. Rates of Evaporation of Water through Compressed Monolayers on Water. *J. Franklin Inst.* **1943**, *235*, 119−162.
(46) Barnes, G. T. Permeation through Monolayers. *Colloids Surf., A* **1997**, *126* (2−3), 149−158.
(47) Van Loon, L. L.; Minor, R. N.; Allen, H. C. Structure of Butanol and Hexanol at Aqueous, Ammonium Bisulfate, and Sulfuric Acid Solution Surfaces Investigated by Vibrational Sum Frequency Generation Spectroscopy. *J. Phys. Chem. A* **2007**, *111* (31), 7338−7346.
(48) Chen, Y.-Y.; Grace Lee, W.-M. Hygroscopic Properties of Inorganic-Salt Aerosol with Surface-Active Organic Compounds. *Chemosphere* **1999**, *38* (10), 2431−2448.
(49) Andrews, E.; Larson, S. M. Effect of Surfactant Layers on the Size Changes of Aerosol-Particles as a Function of Relative Humidity. *Environ. Sci. Technol.* **1993**, *27* (5), 857−865.
(50) Wills, J. B.; Knox, K. J.; Reid, J. P. Optical Control and Characterisation of Aerosol. *Chem. Phys. Lett.* **2009**, *481* (4−6), 153−165.
(51) Tang, I. N. Chemical and Size Effects of Hygroscopic Aerosols on Light Scattering Coefficients. *J. Geophys. Res.* **1996**, *101* (D14), 19,245−19,250.
(52) Dluhy, R. A. Quantitative External Reflection Infrared Spectroscopic Analysis of Insoluble Monolayers Spread at the Air-Water Interface. *J. Phys. Chem.* **1986**, *90* (7), 1373−1379.
(53) Gericke, A.; Michailov, A. V.; Hühnerfuss, H. Polarized External Infrared Reflection-Absorption Spectrometry at the Air/Water Interface: Comparison of Experimental and Theoretical Results for Different Angles of Incidence. *Vib. Spectrosc.* **1993**, *4* (3), 335−348.
(54) Malde, A. K.; Zuo, L.; Breeze, M.; Stroet, M.; Poger, D.; Nair, P. C.; Oostenbrink, C.; Mark, A. E. An Automated Force Field Topology Builder (Atb) and Repository: Version 1.0. *J. Chem. Theory Comput.* **2011**, *7* (12), 4026−4037.
(55) Berendsen, H. J. C.; Postma, J. P. M.; van Gunsteren, W. F.; Hermans, J., Interaction Models for Water in Relation to Protein Hydration. In *Intermolecular Forces*; Pullman, B., Ed.; D. Reidel Publishing Company: Dordrecht, The Netherlands, 1981; pp 331−342.
(56) Byrd, R. H.; Lu, P. H.; Nocedal, J.; Zhu, C. Y.; Limited Memory, A. Algorithm for Bound Constrained Optimization. *SIAM J. Sci. Comput.* **1995**, *16* (5), 1190−1208.
(57) Zhu, C. Y.; Byrd, R. H.; Lu, P. H.; Nocedal, J. Algorithm 778: L-Bfgs-B: Fortran Subroutines for Large-Scale Bound-Constrained Optimization. *ACM Trans. Math. Software* **1997**, *23* (4), 550−560.
(58) Berendsen, H. J. C.; Postma, J. P. M.; Vangunsteren, W. F.; Dinola, A.; Haak, J. R. Molecular Dynamics with Coupling to an External Bath. *J. Chem. Phys.* **1984**, *81* (8), 3684−3690.
(59) Van Der Spoel, D.; Lindahl, E.; Hess, B.; Groenhof, G.; Mark, A. E.; Berendsen, H. J. C. Gromacs: Fast, Flexible, and Free. *J. Comput. Chem.* **2005**, *26* (16), 1701−1718.
(60) Knobler, C. M.; Desai, R. C. Phase-Transitions in Monolayers. *Annu. Rev. Phys. Chem.* **1992**, *43*, 207−236.
(61) Kaganer, V. M.; Mohwald, H.; Dutta, P. Structure and Phase Transitions in Langmuir Monolayers. *Rev. Mod. Phys.* **1999**, *71* (3), 779−819.
(62) Riviere, S.; Henon, S.; Meunier, J.; Schwartz, D. K.; Tsao, M. W.; Knobler, C. M. Textures and Phase-Transitions in Langmuir Monolayers of Fatty-Acids - a Comparative Brewster-Angle Microscope and Polarized Fluorescence Microscope Study. *J. Chem. Phys.* **1994**, *101* (11), 10045−10051.
(63) Kaganer, V. M.; Peterson, I. R.; Kenn, R. M.; Shih, M. C.; Durbin, M.; Dutta, P. Tilted Phases of Fatty-Acid Monolayers. *J. Chem. Phys.* **1995**, *102* (23), 9412−9422.
(64) Knobler, C. M. Seeing Phenomena in Flatland - Studies of Monolayers by Florescence Microscopy. *Science* **1990**, *249* (4971), 870−874.
(65) Moore, B. G.; Knobler, C. M.; Akamatsu, S.; Rondelez, F. Phase Diagram of Langmuir Monolayers of Pentadecanoic Acid - Quantitative Comparison of Surface Pressure and Fluorescence Microscopy Results. *J. Phys. Chem.* **1990**, *94* (11), 4588−4595.
(66) Griffith, E. C.; Adams, E. M.; Allen, H. C.; Vaida, V. Hydrophobic Collapse of a Stearic Acid Film by Adsorbed L-Phenylalanine at the Air-Water Interface. *J. Phys. Chem. B* **2012**, *116* (27), 7849−7857.

(67) Minofar, B.; Jungwirth, P.; Das, M. R.; Kunz, W.; Mahiuddin, S. Propensity of Formate, Acetate, Benzoate, and Phenolate for the Aqueous Solution/Vapor Interface: Surface Tension Measurements and Molecular Dynamics Simulations. *J. Phys. Chem. C* **2007**, *111* (23), 8242−8247.
(68) Mitchell, M. L.; Dluhy, R. A. In Situ Ft-Ir Investigation of Phospholipid Monolayer Phase Transitions at the Air-Water Interface. *J. Am. Chem. Soc.* **1988**, *110* (3), 712−718.
(69) Sierra-Hernandez, M. R.; Allen, H. C. Incorporation and Exclusion of Long Chain Alkyl Halides in Fatty Acid Monolayers at the Air-Water Interface. *Langmuir* **2010**, *26* (24), 18806−18816.
(70) Safran, S. A.; Robbins, M. O.; Garoff, S. Tilt and Splay of Surfactants on Surfaces. *Phys. Rev. A* **1986**, *33* (3), 2186−2189.